The Journal of Experimental Biology 216, 952-959

doi:10.1242/jeb.072710

RESEARCH ARTICLE

Effect of fluid viscosity on the liquid-feeding flow phenomena of a female mosquito

Bo Heum Kim[1,4], Hojin Ha[2,4], Eun Seok Seo[3,4] and Sang Joon Lee[1,2,3,4,*]

[1]School of Interdisciplinary Bioscience and Bioengineering, Pohang University of Science and Technology, Pohang Gyeongbuk, Republic of Korea, [2]Department of Mechanical Engineering, Pohang University of Science and Technology, Pohang Gyeongbuk, Republic of Korea, [3]Division of Integrative Biosciences and Biotechnology, Pohang University of Science and Technology, Pohang Gyeongbuk, Republic of Korea and [4]Center for Biofluid and Biomimic Research, Pohang University of Science and Technology, Pohang Gyeongbuk, Republic of Korea

*Author for correspondence (sjlee@postech.ac.kr)

SUMMARY

Liquid-sucking phenomena by the two-pump system of female mosquitoes were investigated to understand the feeding mechanism. In most previous experimental studies on liquid-feeding insects, the net increase of mass was divided by the feeding time and fluid density to evaluate the intake rate. However, this weighting method is not so precise for mosquitoes, because they are too lightweight to measure the gain of mass accurately. In this study, the intake rate of female mosquitoes feeding on various sucrose solutions was estimated using a micro-particle image velocimetry technique. As the sucrose concentration increased from 1% to 50%, the intake rate decreased from 17.3 to 5.8 nl s^{-1}. In addition, the temporal volume variations of the two pump chambers were estimated based on the velocity and acceleration information of the flow at the center of the food canal of the proboscis. One pumping period was divided into four elementary phases, which are related to the different operational modes of the two pumps. According to the hypothetical model established in this study, the phase shift (α) between the two pump chambers increases from 14 to 28 ms and the percentage of reverse flow to forward flow in a pumping period decreases from 7.6% to 1.7% with increasing viscosity. The developed analytical methodology thus aids in the study of an insect's feeding mechanism.

Key words: liquid-feeding mosquito, micro-PIV, viscous liquid, intake rate.

Received 19 March 2012; Accepted 31 October 2012

INTRODUCTION

Some insects use muscular pumps to take in liquid through their mouthparts. As the airtight pump chamber expands by contraction of its dilator muscles, a large pressure gradient is developed along the proboscis (Borrell, 2006). Among several liquid-feeding insects, the female mosquito sucks nectar for basal metabolism and blood for providing proteins to her eggs (Kingsolver and Daniel, 1995). Mosquitoes operate two pumps inside their head systematically to suck liquid from the outside into their digestive organs: the cibarial dilator pump (CP) and the pharyngeal dilator pump (PP) (Schiemenz, 1957). The blood-sucking mechanism of female mosquitoes has recently been investigated experimentally. Kikuchi and Mochizuki visualized the flow in the proboscis of a mosquito using micro-particle image velocimetry (micro-PIV) (Kikuchi and Mochizuki, 2008). Lee and colleagues studied the transport of blood sucked into the food canal of female mosquitoes using a micro-PIV velocity field measurement technique (Lee et al., 2009). Kikuchi and Mochizuki visualized the blood flow around the proboscis tip and measured the electrical signals generated from the pump muscles located in the mosquito's head (Kikuchi and Mochizuki, 2011). Kim and colleagues visualized the systaltic motion of the two pumps using a synchrotron X-ray micro-imaging technique (Kim et al., 2011a). Kim and colleagues visualized the three-dimensional morphological structure of the pump system of a female mosquito using synchrotron X-ray microscopic computed tomography (Kim et al., 2012).

In previous studies of insect feeding, fluid viscosity was one of the main parameters considered because it changes the power required to operate the pump system. The intake flow rate is known to be altered according to the viscosity of the feeding fluid. Smith investigated the effect of diet viscosity on the operation of the pharyngeal pump in blood-feeding bugs with one pump (Smith, 1979). In contrast to the previous hypothesis of a central nervous system 'oscillator' controlling the pump muscles independently, he proposed that pump muscles are controlled by peripheral feedback from the stretch receptor. The stroke volume and intake rate of the bug decrease as the diet viscosity increases. This tendency is consistent with the feeding of most insects, because feeding rate is inversely proportional to viscosity under constant mean pressure according to Poiseuille's equation. In addition, the feeding frequency of *Rhodnius prolixus*, a liquid-feeding insect, decreases linearly with increasing viscosity of the liquid (Smith, 1979). It would therefore be interesting to investigate whether these relationships work for the two-pump system of a female mosquito. Daniel and colleagues numerically simulated the nectar uptake of butterflies and reported the existence of a certain optimal nectar concentration for maximum intake (Daniel et al., 1989). May empirically calculated the optimal sucrose concentration range at which the rate of energy intake is maximized for two butterfly species (May, 1985). Kim and colleagues investigated the optimal sugar concentrations at which the energy intake rate became maximum for various nectar feeders (Kim et al., 2011b).

We investigated the effect of fluid viscosity on the liquid feeding of female mosquitoes by measuring the intake rate through the food canal using a micro-PIV technique. Intake rate and stroke volume

were estimated with varying sucrose concentrations. In most previous experimental studies on liquid-feeding insects, the intake rate of the ingested fluid was evaluated by measuring the insect's mass before and immediately after feeding. Stroke volume can be calculated by dividing the rate of intake of a food mass by the pumping frequency acquired from an electronic signal. Electronic signals have previously been utilized to measure the operation of a liquid-feeding insect's pump system (Kashin, 1966; Kikuchi and Mochizuki, 2011; Pappas, 1988). However, the mass measurement causes errors with mosquitoes because these insects are too light to measure their mass precisely. In the current study, therefore, intake rate and pumping frequency were estimated simultaneously without obtaining the mass of the test mosquito.

Furthermore, measurement of flow in the food canal is an indirect way of estimating the volumetric variation of the pumping chambers. In previous studies, operation of an insect's pump was mostly estimated based on anatomical observation or the electronic signal from the muscle activity of the pumping organs. Patton and Cragg proposed that the two pumps expand simultaneously to generate enough suction force (Patton and Cragg, 1913). Based on an anatomical observation, Schiemenz hypothesized that the two pumps operate out of phase (Schiemenz, 1957). Pappas also showed that the two pumps are out of phase in the initial contraction, but then change to a more in-phase behavior (Pappas, 1988). Kim and colleagues visualized the systaltic motion of the two pumps in detail using a synchrotron X-ray imaging technique and found that the two pumps work systematically with a certain phase shift (Kim et al., 2011a). In the present study, the temporal volume variations of the two pump chambers of female mosquitoes were estimated according to experimental information acquired from *in vivo* flow measurements. Based on the experimental data and theoretical analysis, a hypothetical model was established to estimate the phasic operation of the two pump chambers in one pumping cycle. Using this approach, the variations of phase shift and rate of reverse flow to forward flow according to sucrose concentration were compared.

MATERIALS AND METHODS

Mosquito sample preparation

Mosquitoes (*Aedes togoi*, Theobald 1907) were reared and maintained in a temperature-controlled room at 27°C, 80% relative humidity (RH), with a 16 h:8 h light:dark photoperiod. Larvae were hatched in distilled water and fed a slurry of ground fish food and baker's yeast with a constant supply of 10% sucrose. Body size is usually determined by larva density in the breeding vat. If larva density is high, the sample size becomes small and *vice versa*. To test female mosquitoes of similar size, larva density was maintained at a fixed level and test samples were picked from the same breeding vat. After pupation, mosquitoes were transferred to a fine-mesh net cage. Upon emergence, a 10% sucrose-soaked cotton rod was supplied from the bottom of the cage. Mosquitoes more than 4 days post-emergence were selected as test samples in this study. More than 100 female mosquitoes were tested to acquire experimental data for each sucrose concentration. However, the success rate for obtaining valuable data was less than 10%. The liquid-feeding phenomenon for each sucrose concentration was recorded for a few seconds. A female mosquito was glued on a glass slide with instant glue and a certain amount of feeding liquid was supplied at the tip of the proboscis. The mosquito samples were starved for 1 day before the experiment.

The mouthpart (proboscis) of a mosquito consists of six piercing slender stylets appressed in a fascicle and one wrapping organ. Among the six piercing stylets, the labrum working as the food canal is the largest and stiffest stylet in the fascicle (Clements, 1992). The wrapping organ, the labium, has a feather-like opaque cuticle that prevents the observation of blood flow through the food canal. To visualize the blood flow inside the food canal and apply a PIV technique, the opaque cuticle of the proboscis was removed by microsurgery. To record flow images at the one-quarter location of the food canal from the tip, about half of the cuticle was stripped off using keen-edged forceps. After this treatment, the food canal became translucent (Kim et al., 2011a).

Micro-PIV technique

Fig. 1 shows a schematic diagram of the experimental set-up used in this study. A micro-PIV velocity field measurement technique was employed to measure the variation in the streamwise velocity of blood flow in the food canal of a mosquito (Kikuchi and Mochizuki, 2008; Lee et al., 2009). The micro-PIV system consists of a vertical microscope (Eclipse 80i, Nikon, Nishiohi, Tokyo, Japan), a continuous Nd:YAG laser (λ=532 nm) as a light source, a high-speed CMOS camera (Photron ultima APX, Fujimi, Tokyo, Japan) and a PC for data processing and control. Images were captured consecutively at a frame rate of 10,000 frames s^{-1} using the high-speed camera. The spatial resolution of the PIV system was about 1 μm $pixel^{-1}$ and the field of view was 256×256 μm. The width of the food canal corresponds to about 30 pixels. To calculate the centerline velocity inside the food canal, we cropped the raw

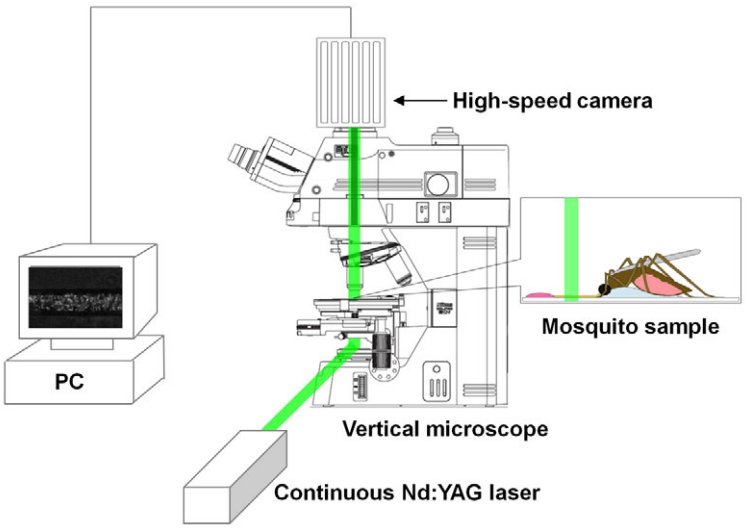

Fig. 1. Schematic diagram of the micro-particle image velocimetry (PIV) system used for investigating fluid feeding of a female mosquito.

particle image to 256×6 pixels at the center region of the food canal. The consecutive images were cross-correlated to calculate the centerline velocity. The optical aberration in particle images due to the mismatch in refractive indices has little influence on the velocity measurements because the wall thickness of the food canal is only a few micrometers (Kikuchi and Mochizuki, 2008) and only the narrow center region is cropped to estimate the centerline velocity. To enhance the signal-to-noise ratio in the correlation planes, the mean intensity of the surrounding region was subtracted from the intensity distribution of each interrogation region. Time-resolved velocity at the center region of the food canal was obtained by applying a fast Fourier transform (FFT)-based cross-correlation PIV algorithm to the consecutive flow images. The depth of focus of the present experimental set-up was about 15 μm. Therefore, the estimated velocities would be slightly biased because of the limited depth of focus, because the entire food canal was illuminated by a volume of laser. The maximum velocity estimated at the center of the food canal may be underestimated for the experimental set-up used in this study (Kloosterman et al., 2011). Mosquitoes were fed sucrose solutions of 1%, 30% and 50% (weight/weight) concentration. The viscosity of each sucrose solution was measured at 25°C using a digital viscometer (Brookfield DV-II+Pro, Brookfield Engineering Laboratory Instruments, Middleboro, MA, USA; see Table 1). Sucrose solution was mixed with fluorescent tracer particles made of polystyrene (Molecular Probes, Eugene, OR, USA) with a mean diameter of 1.0 μm (1.0×10^9 ml^{-1}) and then placed near the tip of the mosquito's proboscis. The fluorescent particles absorb green light at a peak wavelength of λ=534 nm and emit light at a peak wavelength of λ=554 nm. Fluorescent images of tracer particles were captured through a high-pass filter (λ=550 nm) attached to the microscope. The traceability of tracer particles to a flow is usually estimated by the particle Stokes number S, defined as follows.

$$S = \frac{\rho_p r_p^2 u}{\mu D} , \quad (1)$$

where ρ_p and r_p are the density and radius of the particle, respectively. u and μ are the velocity and viscosity of the flow, respectively. D is the diameter of the food canal. In the present study, S is 1.0×10^{-2}, much smaller than 1. This implies that the particles follow the flow substantially (Hirono et al., 2008). During the experiments, temperature and RH inside the air-conditioned room were maintained at 25°C and 45%, respectively.

Data processing

Fig. 2 summarizes the phase-averaging process employed in the present study. Temporal variation of the streamwise velocity signal was extracted from consecutive flow images at the center of the food canal (Fig. 2A). The velocity signal was filtered with a cut-off frequency of 100 Hz. Large velocity fluctuations were observed during high-speed liquid intake (Fig. 2B). Velocity signals at the center of the food canal were phase averaged to evaluate the operational features of the two pump chambers (Fig. 2C). Four pumping cycles were phase averaged to evaluate the average pumping cycle. The phase-averaged velocity signals show a typical pumping behavior in a cycle. They were obtained by ensemble averaging of the instantaneous velocity signal as a function of phase angle for four feeding cycles of each mosquito sample. To provide the same number of data points at each cycle in this phase averaging, the interpolation method using piecewise polynomial expression between adjacent data was employed. If we consider a fully developed Poiseuille flow in a round pipe of diameter D, by applying the momentum equation to a control volume, the intake flow rate ($\dot{Q}$) can be evaluated using the following equation:

$$\dot{Q} = \frac{\pi}{8} D^2 V_C , \quad (2)$$

where D is the diameter of the food canal and V_C is the velocity signal at the center of the food canal. Flow acceleration was calculated by differentiating V_C with respect to time. In this research, we assumed that the food canal has a circular cross-section because it is difficult to measure the exact shape of the cross-section. However, the food canal actually has a non-circular cross-section, and therefore the results will be slightly different from the real values (Kikuchi and Mochizuki, 2008). Stroke volume of a mosquito can be estimated either by dividing the average intake flow rate by the pumping frequency or by integrating the intake flow rate over one pumping cycle. In this study, the latter estimation method was adopted. The pumping frequency is the reciprocal of the pumping period.

Statistical analysis

Experimental data were obtained from five mosquitoes for each concentration of sucrose solution. The performance of different groups was compared using one-way ANOVA followed by Tukey's *post hoc* test with Minitab 16.1.0 program. $P<0.05$ was used to illustrate statistical significance.

RESULTS AND DISCUSSION

Typical temporal variation of intake rate and acceleration

Fig. 3 shows the typical temporal variation of intake flow rate and the corresponding flow acceleration estimated inside the food canal during one pumping period. In Fig. 3A, steep changes of intake rate occur at the phases around t/T of 0.28 and 0.74. The time t is normalized by the period T of one liquid-feeding cycle. The average intake rate during the initial t/T time periods 0–0.28 and 0.28–0.83 is ~5.8 and 47.2 nl s^{-1}, respectively. The high intake rate rapidly decreases around t/T=0.74 and then a slight reversal intake flow is observed during the t/T time period of 0.83–1.00. The average reversal intake flow is approximately −5.9 nl s^{-1}. This intake pattern is periodically repeated throughout the whole liquid-feeding process.

Table 1. Parametric values related to the operation of the two pumps according to the sucrose concentration

Concentration (%)	Viscosity (cP)	Phase 1 (ms)	Phase 2 (ms)	Phase 3 (ms)	Phase 4 (ms)	$\dot{Q}_2/\dot{Q}_1$ (%)	V_4/V_{1-3} (%)
1	1.5	44±6	78±6	14±3	27±5	6.3±1.1	7.6±1.4
30	2.7	32±9	70±3	19±2	16±3	5.6±1.3	4.3±1.4
50	13.0	52±16	73±6	28±4	17±6	2.9±0.7	1.7±1.2

Phase 3 corresponds to the phase shift (α) between the operation of the cibarial dilator pump (CP) and the pharyngeal dilator pump (PP).
$\dot{Q}_2/\dot{Q}_1$ is the ratio of intake rate during phase 2 with respect to phase 1.
V_{1-3} and V_4 are the intake volume from phase 1 to phase 3, and phase 4, respectively.
All values are indicated as means ± s.e.m.

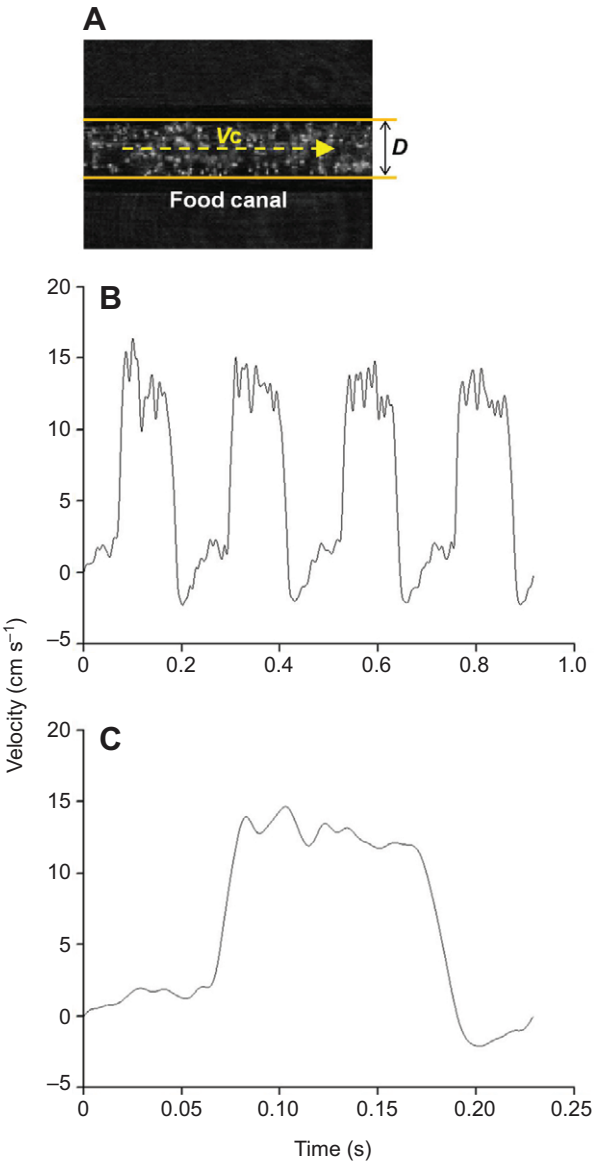

Fig. 2. The phase-averaging process employed in this study. (A) Typical flow images, (B) streamwise velocity signal acquired at the center of the food canal and (C) phase-averaged velocity signal. In the consecutive flow images captured with a high-speed camera, only a 6 pixel-width center region of the food canal was used to extract the time-resolved velocity vectors using a fast Fourier transform (FFT)-based cross-correlation PIV algorithm. V_C, velocity at the center of the food canal; D, diameter of the food canal.

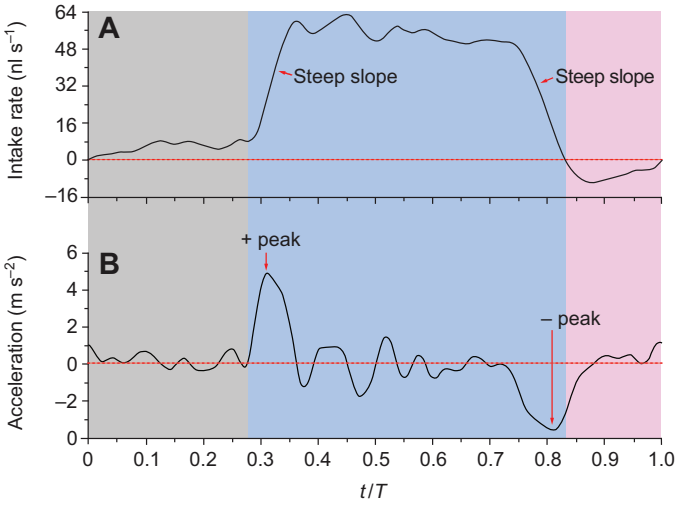

Fig. 3. (A) Temporal variations of intake flow rate inside the food canal of a female mosquito and (B) the corresponding flow acceleration. One pumping cycle is divided into three domains (shaded regions) based on the intake rate. The average intake rate ($\dot{Q}_{avg}$) for the low (gray), high (blue) and reversal (pink) flow domains is 5.8, 47.2 and –5.9 nl s^{-1}, respectively. The positive (+) and negative (–) acceleration peaks are indicated. The time t is normalized by the period T of one liquid-feeding cycle.

Two acceleration peaks can be seen in Fig. 3B. The first peak has a positive value and the second peak has a negative value. The acceleration signal exhibits the maximum positive and negative value at t/T=0.31 and 0.81, respectively. These peaks in the acceleration signal coincide well with the instants of rapid change in intake rate. From these results, we can see that the positive and negative acceleration peaks are closely related to the rapid increase and decrease of intake rate, respectively.

Viscosity effect on the liquid intake of a female mosquito

Intake rate was estimated with varying concentrations of sucrose solutions to evaluate the effect of viscosity on the liquid intake of a female mosquito. Fig. 4 shows the intake rate and stroke volume for three sucrose concentrations: 1%, 30% and 50%. With increasing sucrose concentration, both viscosity and sweetness are increased. Borrell investigated the feeding of sucrose solution in a bee and found that the intake rate was dependent on the viscosity but not the sweetness of the sucrose solution (Borrell, 2006). In this study, the intake rates obtained for 1%, 30% and 50% (w/w) sucrose solutions were 17.3±2.6, 14.3±4.3 and 5.8±1.4 nl s^{-1} (means ± s.e.m.), respectively. The intake rates are significantly different between groups (ANOVA; $F_{2,12}$=3.97, P<0.05). A *post hoc* Tukey test was performed and the results show that the intake rate for 50% sucrose solution is significantly lower than that for 1% sucrose solution (P<0.05). However, there are no significant differences in intake rate for the ranges of sucrose concentration between 1% and 30% and between 30% and 50% (P>0.05). On an average, the intake rate of 50% sucrose is about 34% that of 1% sucrose. This decrease of intake rate with high sucrose concentration may be attributed to the decrease in stroke volume (intake volume per stroke) or pumping frequency. To investigate the effects of viscosity on the intake flow phenomena systematically, the stroke volume and the pumping frequency need to be controlled separately, because the average intake rate in a pumping cycle can be estimated by their product. The pumping frequency was found to be 6.4±0.6, 7.6±0.7 and 6.2±0.7 Hz (means ± s.e.m.) during the intake of 1%, 30% and 50% solutions, respectively. No significant difference in the pumping frequency was detected among the concentrations tested in this study (ANOVA; $F_{2,12}$=1.29, P=0.311). The stroke volume obtained for 1%, 30% and 50% sucrose solutions was 2.2±0.1, 1.6±0.2 and 0.9±0.2 nl, respectively. The stroke volumes are not significantly different between group (ANOVA; $F_{2,12}$=3.62, P=0.059). These results imply that both pumping frequency and stroke volume contribute to the decrease of intake rate with increasing sucrose concentration from 1% to 50%.

Flow acceleration and pumping frequency

The dramatic increase and decrease in acceleration implies that considerable force is induced on the pump chambers. In the

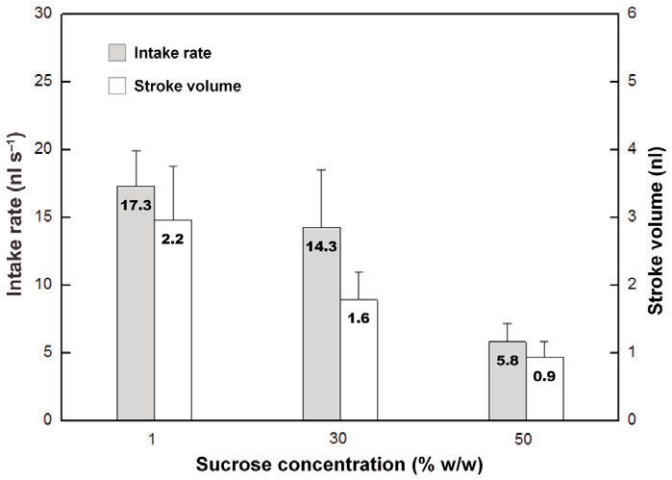

Fig. 4. Intake rate and stroke volume according to sucrose concentration. Data are means and s.e.m.

muscular pump of an insect, the pressure drop can be estimated simply by dividing the muscular force by the cross-sectional area of the muscles (Kingsolver and Daniel, 1995). For a Poiseuille flow, the intake rate ($\dot{Q}$) passing through a pipe is proportional to the pressure drop (ΔP) along the pipe. Flow acceleration is proportional to the rate of change of intake rate with time according to Eqn 2. Therefore, the rapid change in flow acceleration can be assumed to be caused by the change of force acting on the pump chambers. Kikuchi and Mochizuki found that the acceleration of red blood cells sucked up by a mosquito was almost synchronized with the increase of the electromyogram signal amplitude from a mosquito's pump muscle (Kikuchi and Mochizuki, 2011).

In general, the intake rate of insects decreases as the viscosity of the feeding fluid increases (Borrell, 2006; Falibene et al., 2009; Smith, 1979). Smith showed that the increase of fluid viscosity decreased both the feeding frequency and the average stroke volume of an assassin bug (Smith, 1979). However, the pumping frequency of insects does not show a consistent trend with respect to the increase of fluid viscosity. In the case of the carpenter ant, the pumping frequency does not vary significantly as the viscosity of the feeding fluid increases (Falibene et al., 2009). The present results also do not show a clear relationship between the pumping frequency and the viscosity of feeding fluid.

Hypothetical analysis of the two-pump system

Four elementary phases of the liquid-sucking process

A hypothetical model for the two-pump system was established to elucidate the relationship between flow in the food canal and volume variations of the pump chambers in the head. It is based on the experimental data on the flow inside the proboscis and theoretical analysis of the cyclic volume variations of CP and PP with a phase shift (see Appendix and Fig. A1). Intake flow rate is closely related to the volume variation of the pump chambers. A large pump volume leads to a high intake rate and *vice versa*. In Fig. 5A, the steep change of intake rate indicates that the volume of the pump chambers varies greatly. A negative intake rate denotes that both pump chambers are contracting. The acceleration signal of Fig. 5B shows zero-crossing points where the acceleration signal crosses the *x*-axis. These zero-crossing points indicate the instants at which the pump chambers start to expand or contract. They were used as reference points to apply the same standard to all data in this study. Fig. 5C shows the temporal volume variation of CP and PP, modeled based on flow information. The pump volume is illustrated in arbitrary units without the exact volume variation information from each pump.

One pumping cycle is divided into four phases, based on the change of intake rate and flow acceleration. Phase 1 corresponds to the initial period during which the CP takes in liquid from the outside into the pumping organs through the food canal. In this phase, the anterior pharyngeal valve, located between the two pump organs, is considered to be closed. The initiation of phase 2 is determined by the zero-crossing of the positive acceleration peak (Fig. 5B). The intake rate increases rapidly when the pumping period changes from phase 1 to phase 2, which is due to the large expansion of the PP. The intake rate in phase 1 is caused by CP expansion only, whereas that of phase 2 results from the expansion of both the CP and PP.

The PP starts to expand in advance, with a time (β) corresponding to the duration of phase 2. The flow rate jumps in proportion to the volumetric amplitude of the PP (see Appendix and Fig. A1). The large jump of flow rate shown in phase 2 indicates that the volume variation of the PP is much larger than that of the CP. In this model, the effect of PP expansion can be evaluated using the ratio ($\dot{Q}_2/\dot{Q}_1$) of the intake rate between phase 1 ($\dot{Q}_1$) and phase 2 ($\dot{Q}_2$). The ratio $\dot{Q}_2/\dot{Q}_1$ is not significantly different between groups (ANOVA; $F_{2,12}$=2.65, P=0.111; see Table 1).

The initiation of phase 3 is determined by the zero-crossing of the negative acceleration peak (Fig. 5B). In phase 3, the maximum expansion of the two pump organs has a definite phase shift (α). In the final phase, phase 4, the PP pushes the liquid posteriorly (toward the body) and the CP discharges the remaining fluid anteriorly (toward the food canal), causing the reversal of flow in the food canal. In our model, in the final phase the anterior pharyngeal valve is closed to prevent the reverse flow from the PP to the CP. The theoretical intake rate profile obtained by assuming that the anterior pharyngeal valve closes in phase 4 is well matched with the *in vivo* results. In this study, the anterior pharyngeal valve is considered to be open in phase 2 and phase 3, during which the PP draws liquid from the CP. On average, phase 2 and phase 3 accounted for about 62% of all phases in one pumping period. This percentage does not change significantly as the concentration of sucrose solution increases (ANOVA; $F_{2,12}$=0.86, P=0.448).

Relationship between α and reverse flow

Fig. 6 shows variations of α and the ratio of reverse flow to forward flow for the three sucrose concentrations (1%, 30% and 50%). Here, α increases as the concentration of the sucrose solution increases (14±3, 19±2 and 28±4 ms, means ± s.e.m. for 1%, 30% and 50%). The α values are significantly different between groups (ANOVA; $F_{2,12}$=5.42, P<0.05). Tukey's *post hoc* test was performed and the results show that α for 50% sucrose solution is significantly longer than that for 1% sucrose solution (P<0.05). However, there is no significant difference in α for the range of sucrose concentrations between 1% and 30% and between 30% and 50% (P>0.05). The α value for 50% sucrose is about 100% longer than that of the 1% solution. The increase of α implies an increase of the expansion period of the PP while the CP contracts. This cross-operational mode reduces the reverse flow inside the food canal when the CP contracts. The ratio of reverse flow to forward volume flow ($V_4/V_{1–3}$, $V_{1–3}$ is the forward volume flow in the period from phase 1 to phase 3, and V_4 is the reverse flow in phase 4), is expected to decrease as the phase shift increases. The ratio $V_4/V_{1–3}$ is significantly different between groups (ANOVA; $F_{2,12}$=4.75, P<0.05, see Table 1). The *post hoc* Tukey test shows that $V_4/V_{1–3}$

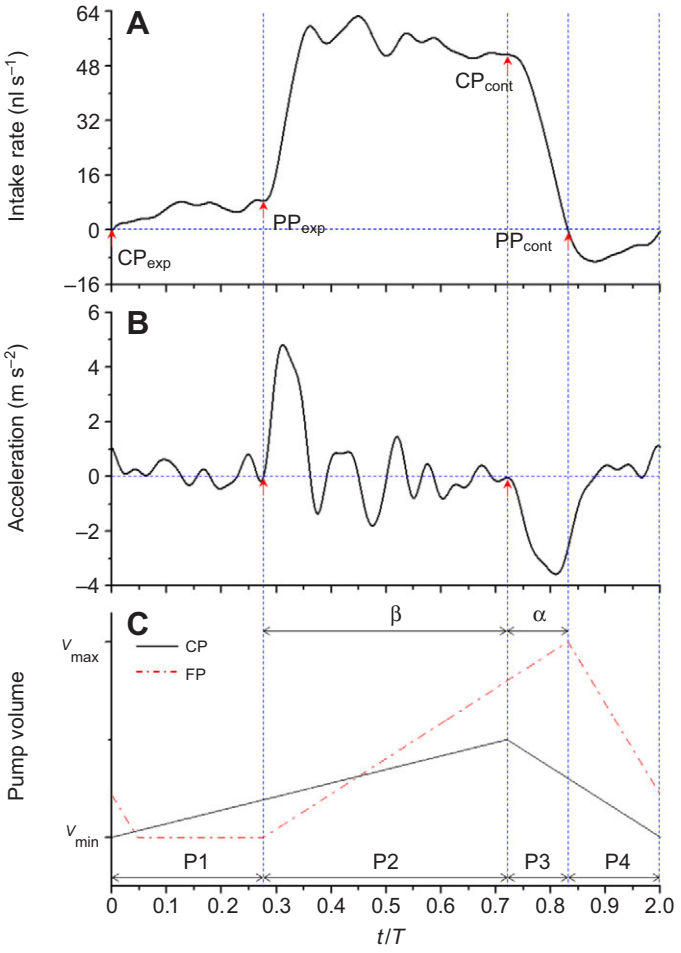

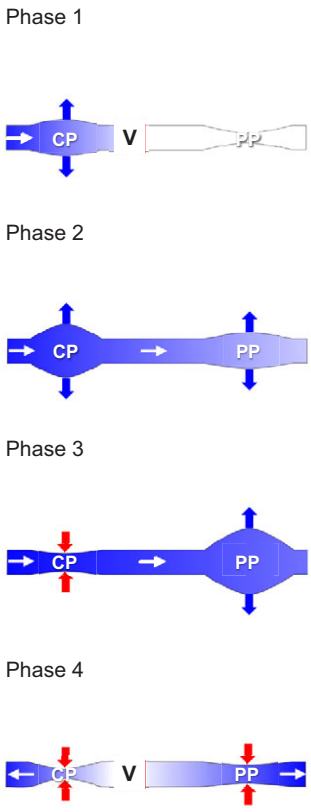

Fig. 5. (A) Temporal variations of intake flow rate inside the food canal of a female mosquito and (B) the corresponding acceleration and (C) hypothesized model for the volume variation of the two pumping organs. The hypothesis of the liquid-feeding process was based on the modeled volume variations of individual pump chambers. CP_{exp} and PP_{exp} denote the expansion of the cibarial dilator pump (CP) and the pharyngeal dilator pump (PP), respectively. CP_{con} and PP_{con} denote the contraction of the CP and PP, respectively. Red arrows indicate the zero-crossing point of the marked acceleration peak. α, phase shift; β, expansion time of the PP; P1–P4, phase 1–4 of the pumping cycle. In the right-hand panels, the anterior pharyngeal valve used to close the flow path between the CP and PP is indicated by v; horizontal and vertical arrows indicate the flow direction and pump chamber motion, respectively.

for the 50% sucrose solution is significantly smaller than that for the 1% sucrose solution (P<0.05). However, there is no significant difference in $V_4/V_{1–3}$ for the ranges of sucrose concentration between 1% and 30% and between 30% and 50% (P>0.05). Multi-functional performance is also possible because of the phase shift between the operation of the two pump chambers during phase 1. In this phase, CP takes in liquid through the food canal while PP transports the food to the digestive organs by passing the posterior pharyngeal valve.

Relationship between CP volume and PP expansion

For blood flow in the human heart, it is of great interest to consider the relationship between ventricular volume and intraventricular pressure during diastole phase. Until the ventricular volume reaches a certain value, the diastolic pressure does not increase greatly. When the volume is increased above the threshold value, the diastolic pressure increases rapidly because the pericardium surrounding the heart is stretched nearly to its limit. The high pressure in the ventricle is used to pump the blood to the whole body (Guyton and Hall, 1996). This operational behavior of the ventricular volume with respect to the inner pressure can be similarly applied to the two pump chambers of a female mosquito. For liquid-feeding female mosquitoes, when the CP volume is increased above a threshold volume, the pressure inside the chamber increases considerably to transport the liquid feed to the PP easily. The intake volume of the CP during phase 1 (V_1) was measured to check whether the CP volume reaches a certain value just before the start of PP expansion. There was no significant difference in V_1 values, irrespective of sucrose concentration tested in this study (ANOVA; $F_{2,12}$=1.12, P=0.359).

Comparison with previous studies on phasic variation

In our previous study using the synchrotron X-ray imaging technique (Kim et al., 2011a), the pumping process was divided into three phases. In contrast to the present study, the PP expansion was not divided into two phases. Pump volume was estimated from the light intensity variation of each pump. However, because the PP has a rather complicated structure compared with the CP, it is difficult to obtain a clear intensity value when the volume variation of the PP is small. X-ray images showing the opening and closing events of each pump chamber were recorded at about 30 frames s^{-1}. However, optical images of flow tracers in the proboscis were acquired at 10 kframes s^{-1}. Phasic variation of the liquid-feeding process was therefore analyzed more precisely compared with previous studies. Moreover, the acceleration peaks newly described in this study provide information on the variation of driving force acting on the pump chambers.

CONCLUSIONS

Female mosquitoes suck both nectar and blood. Nectar and blood have different fluid properties such as viscosity and non-Newtonian characteristics. Therefore, depending on the food it is feeding on, the flow inside the food canal of a female mosquito also differs.

The intake rate of a mosquito according to fluid viscosity was obtained from the velocity signals estimated at the center of the food canal (V_C) using a micro-PIV technique. In addition, flow acceleration was calculated by differentiating V_C with respect to

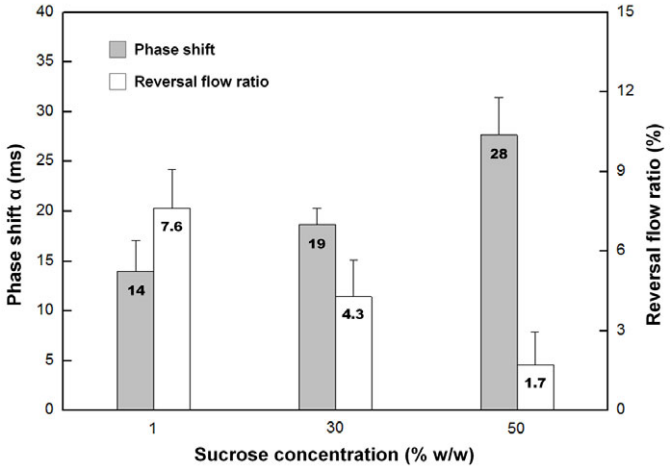

Fig. 6. Phase shift (α) and reverse flow ratio according to sucrose concentration. Reverse flow ratio is the ratio of reverse flow to forward flow. Data are means and s.e.m.

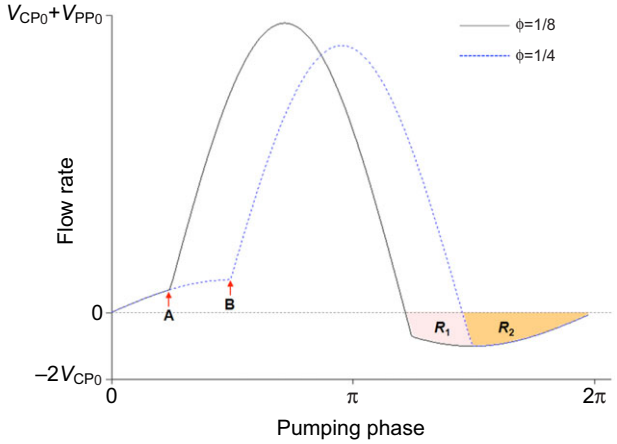

Fig. A1. Phasic variation of flow rate produced by the two pump chambers for which the volume variations are expressed by a cosine function. The rapid increase of flow rate starts earlier for the phase shift of 4/π (=1/8) compared with that of 2/π (=1/4). The volume (R_1+R_2) of reverse flow for a phase shift of 4/π is larger than that of 2/π (R_2).

time. Variations in the temporal volume of the two pump chambers of a female mosquito with several different concentrations of sucrose solution were estimated using a hypothetical model established based on the experimental data and theoretical analysis. We found that the phase shift (α) increases as the sucrose concentration increases. The ratio of reverse flow to forward volume flow decreases with the increase in α.

The experimental methodology developed in this study is especially useful for flow measurements of liquid-feeding insects such as mosquitoes. It is also applicable to the study of the feeding mechanism of other insects that drink liquid through a food canal, such as butterflies, assassin bugs and sucking lice. The establishment in the near future of new advanced experimental methodologies combining flow measurements in the proboscis with direct visualization of the pump organs would aid in the detailed understanding of the pumping mechanism of female mosquitoes.

APPENDIX

Temporal variation of the volume of the two pump chambers (V_{CP} and V_{PP}) of a female mosquito operating with a phase shift (2π ϕ) can be expressed approximately as follows:

$$V_{CP} = V_{CP_0}\left(1-\cos(\omega t)\right), \quad \text{(A1)}$$

$$V_{PP} = V_{PP_0}\left(1-\cos(\omega t - 2\pi\phi)\right), \quad \text{(A2)}$$

where V_{CP} and V_{PP} are the volumetric amplitude of the CP and PP, respectively, ω ($0<\omega<2\pi$) is the angular frequency and 2π ϕ ($0\le\phi\le1/2$) is a phase shift between the two pump chambers. The flow rate induced by each pump chamber ($\dot{Q}_{CP}$ and $\dot{Q}_{PP}$) is equal to the rate of volume change of each pump chamber. Thus:

$$\dot{Q}_{CP} = \frac{dV_{CP}}{dt} = \omega V_{CP_0}\sin(\omega t), \quad \text{(A3)}$$

$$\dot{Q}_{PP} = \frac{dV_{PP}}{dt} = \omega V_{PP_0}\sin(\omega t - 2\pi\phi),\ 2\pi\phi \le \omega \le \pi + 2\pi\phi, \quad \text{(A4)}$$

$$\dot{Q}_{PP} = 0,\ \pi + 2\pi\phi < \omega < 2\pi + 2\pi\phi, \quad \text{(A5)}$$

where $\dot{Q}_{PP}$ is an interval function modified to be zero when the sign of sin(ωt–2π ϕ) becomes negative, in consideration of the valve located between CP and PP (the anterior pharyngeal valve) for preventing reverse flow from the PP to the CP. The phasic variation of theoretical intake rate is well matched by the *in vivo* result, when we assume that the anterior pharyngeal valve is closed in phase 4. The flow rate in the food canal ($\dot{Q}$) of a female mosquito is equal to sum of $\dot{Q}_{CP}$ and $\dot{Q}_{PP}$. Thus:

$$\dot{Q} = \omega V_{CP_0}\sin(\omega t),\ 0 \le \omega < 2\pi\phi,\ \pi + 2\pi\phi < \omega < 2\pi + 2\pi\phi, \quad \text{(A6)}$$

$$\dot{Q} = \omega\left(V_{CP_0}\sin(\omega t) + V_{PP_0}\sin(\omega t - 2\pi\phi)\right),$$
$$2\pi\phi \le \omega \le \pi + 2\pi\phi. \quad \text{(A7)}$$

Fig. A1 shows typical phasic variations of flow rate calculated using Eqns A6 and A7 when the phase shift is 4/π (solid line) and 2/π (dotted line). Here, V_{CP} and V_{PP} are 1 and 8, respectively, and ω is 1. The volume ratio for the maximum volumes of the CP and PP was determined arbitrarily. This represents a steep change of intake rate between phase 1 and phase 2. The rapid increase of flow rate starts earlier for the phase shift of 4/π (point A in Fig. A1), compared with that of 2/π (point B in Fig. A1). Points A and B correspond to the start of PP expansion. In the experimental data, the zero-crossing points can be used as references in determining the temporal volume variation of the two pump chambers. The volume (R_1+R_2) of the reversal flow for a phase shift of 4/π is larger than that of 2/π (R_2).

ACKNOWLEDGEMENTS

We are grateful to Mrs S. H. Park for caring for the experimental insects.

FUNDING

This work was supported by the Creative Research Initiatives (Diagnosis of Biofluid Flow Phenomena and Biomimic Research) of the Ministry of Education, Science and Technology/National Research Foundation of Korea. This research was also supported by the World Class University program through the National Research Foundation of Korea funded by the Ministry of Education, Science and Technology [grant no. R31-2008-000-10105-0].

REFERENCES

Borrell, B. J. (2006). Mechanics of nectar feeding in the orchid bee *Euglossa imperialis*: pressure, viscosity and flow. *J. Exp. Biol.* **209**, 4901-4907.
Clements, A. N. (1992). *The Biology of Mosquitoes*. Oxford: CABI Publishing.
Daniel, T. L., Kingsolver, J. G. and Meyhofer, E. (1989). Mechanical determinants of nectar-feeding energetics in butterflies: muscle mechanics, feeding geometry, and functional equivalence. *Oecologia* **79**, 66-75.
Falibene, A., Gontijo, A. F. and Josens, R. (2009). Sucking pump activity in feeding behaviour regulation in carpenter ants. *J. Insect Physiol.* **55**, 518-524.

Guyton, A. C. and Hall, J. E. (1996). Heart muscle; the heart as a pump. In *Textbook of Medical Physiology* (ed. J. E. Hall), pp. 110-115. Philadelphia, PA: W. B. Saunders Company.
Hirono, T., Arimoto, H., Okawa, S. and Yamada, Y. (2008). Microfluidic image cytometry for measuring number and sizes of biological cells flowing through a microchannel using the micro-PIV technique. *Meas. Sci. Technol.* **19**, 025401.
Kashin, P. (1966). Electronic recording of the mosquito bite. *J. Insect Physiol.* **12**, 281-286.
Kikuchi, K. and Mochizuki, O. (2008). Micro-PIV measurements in micro-tubes and proboscis of mosquito. *J. Fluid Sci. Tech.* **3**, 975-986.
Kikuchi, K. and Mochizuki, O. (2011). Micro-PIV (micro particle image velocimetry) visualization of red blood cells (RBCs) sucked by a female mosquito. *Meas. Sci. Technol.* **22**, 064002.
Kim, B. H., Kim, H. K. and Lee, S. J. (2011a). Experimental analysis of the blood-sucking mechanism of female mosquitoes. *J. Exp. Biol.* **214**, 1163-1169.
Kim, W., Gilet, T. and Bush, J. W. M. (2011b). Optimal concentrations in nectar feeding. *Proc. Natl. Acad. Sci. USA* **108**, 16618-16621.
Kim, B. H., Seo, E. S., Lim, J. H. and Lee, S. J. (2012). Synchrotron X-ray microscopic computed tomography of the pump system of a female mosquito. *Microsc. Res. Tech.* **75**, 1051-1058.
Kingsolver, J. G. and Daniel, T. L. (1995). Mechanics of food handling by fluid-feeding insects. In *Regulatory Mechanism in Insect Feeding* (ed. R. F. Champman), pp. 32-73. New York, NY: Springer.
Kloosterman, A., Poelma, C. and Westerweel, J. (2011). Flow rate estimation in large depth-of-field micro-PIV. *Exp. Fluids* **50**, 1587-1599.
Lee, S. J., Kim, B. H. and Lee, J. Y. (2009). Experimental study on the fluid mechanics of blood sucking in the proboscis of a female mosquito. *J. Biomech.* **42**, 857-864.
May, P. G. (1985). Nectar uptake rates and optimal nectar concentrations of two butterfly species. *Oecologia* **66**, 381-386.
Pappas, L. G. (1988). Stimulation and sequence operation of cibarial and pharyngeal pumps during sugar feeding by mosquitoes (Diptera: Culicidae). *Ann. Entomol. Soc. Am.* **81**, 274-277.
Patton, W. C. and Cragg, F. W. (1913). *A Textbook of Medical Entomology.* Calcutta: Christian Literature Society for India.
Schiemenz, H. (1957). Vergleichende funktionell-anatomische Untersuchungen der Kopfmuskulatur von. *Deutsche Entomologische Zeitschrift* **4**, 268-331.
Smith, J. J. B. (1979). Effect of diet viscosity on the operation of the pharyngeal pump in the blood-feeding bug *Rhodnius prolixus*. *J. Exp. Biol.* **82**, 93-104.